Ethiopian Journal of Business and Social Science
https://doi.org/10.59122/174F53to
Volume: 7 Number: 2, 2024, Pages: 54~81
ISSN: 2707- 2770

# Modeling of Future Land Use Dynamics at Biodiversity Hotspot Area in Southern Part of Ethiopian Rift Valley Lake Basin Using CA-Markov and Intensity Analysis Models

**Mohammed Seid[12*], Belay Simane[1], Ermias Teferi[1], and Asnake Boyana[2]**

[1]*Centre for Environment and Development Studies, Addis Ababa University, Addis Ababa, Ethiopia*
[2]*Department of Geography and Environmental Studies, Arba Minch University, Arba Minch, Ethiopia*
** Concerning this article should be addressed to Mohammed Seid; Email:* mohammed.seidA@aau.edu.et

ARTICLE INFO

*Accepted on: March, 2024*
*Published on: December, 2024*



ABSTRACT

*Despite being crucial to global biodiversity and environmental health, many Protected Areas (PAs), including Nechsar National Park (NNP), which is part of the Somalia-Masai Center of Endemism, experienced a threatening loss of functionality due to continued land conversions and degradation, caused by human and natural drivers. Detailed analysis of Future Land Use Change (FLUC) for PAs is vital to follow up and prevent the potential impacts of disastrous changes on biodiversity and ecosystem services via proactive interventions. This study analyzed the size and intensity of FLUC in NNP, in Ethiopia, using Landsat imageries (1986, 2002, and 2020), four explanatory variables, CA-Markov and intensity analysis models, and GIS software including TerrSet_2020. Kappa Index of Dis/Agreements/ was applied to check the effectiveness of CA-Markov and the result was 0.893 ($K_{standard}$).Concerning the overall change, the study revealed a rapid transition from 2020-2040 and slightly slower from 2040-2060, but still expected to cover 45% of the study area. A continued decline is projected in forest, woodland, and grassland with net losses of 19%, 26%, and &70%, respectively. The most active gain that intensively targeting woodland and grassland is predicted in bush/shrubland, whereas the most active loss is from grassland. Similarly, active loss is anticipated from forest due to intensive displacement by cultivated and woodland. The study highlighted that the predicted intensive transitions can be triggered by change drivers under the concept of uniform intensity.They also have implications in escalating the ongoing ecological problems, unless targeted interventions are implemented to control and reverse them. Additionally, integrating CA-Markov with intensity analysis is crucial to quantify the underlying characteristics of FLUC and provide valuable information for rational policy making.*

***Keywords:*** *biodiversity hotspot, intensive, land transition, Nechsar*

## INTRODUCTION

Biodiversity, the complex diversification of species and ecosystems (Mekonnen, 2022), is indispensable for environmental processes, socioeconomic development, and human survival (Kubiszewski et al.,2017; Winkler et al., 2021). Nevertheless, due to increased human-driven land use change (LUC) and degradation, unprecedented biodiversity loss has been observed worldwide over the last few decades (Feng et al., 2023; Venter et al., 2016). The persistent loss in biodiversity has resulted in multifaceted environmental and socioeconomic problems: climate change, agricultural production decline, and food insecurity (Venter et al., 2016).

Thus, the establishment and adequate management of PAs are essential instruments for sustainable biodiversity conservation and utilization, particularly nowadays, when human activities are posing pervasive and intensive threats to the environment (Marchese, 2015; Venter et al., 2016). In this study, PAs refer to biologically diverse (both flora and Fauna) sites and any geographical areas that are gazetted for protecting biodiversity and restoring critically /endangered/ species and habitats through legal frameworks (Lu et al., 2018). Besides biodiversity conservation and ecological services, PAs are important for sustainable livelihood improvement, diversification, and also ecotourism development, particularly in developing countries, without harming the natural status quo of ecosystems (Cunha et al., 2021; Mekonnen, 2022). Accordingly, the number and area of PAs have increased, and today, there are more than 155,584 PAs, covering 12.5% of the Earth's surface (Jin & Fan, 2018).

Although the number and areas are advancing, PAs across the globe have been under pressing habitat (ecosystems) degradation and biodiversity loss due to increased land transition to cultivated and settlement areas, commercial farms and livestock grazing, and over-exploitation of natural forests for the demand of fuel and construction materials (Bailey et al., 2015; Lu et al., 2018; Marchese, 2015). Linked with high population growth and prevalence of natural resources-based subsistence economy, LUC and the resulting impacts have been more pervasive and worsened at PAs located in developing countries (Bailey et al., 2015), including Ethiopia (Temesgen et al., 2022); although the highest biodiversity and PAs concentration of the world are found in these countries (Naughton-Treves et al.,2005). For example,in Savannah, Africa, more than 82% of biodiversity conservation areas have been under the state of failure, which is mainly attributed to deforestation and land degradation because of persistent and daunting socioeconomic pressures from local communities coupled with administration problems (Robsonetal.,2022).Thus, quantifying and mapping the trends and patterns of LUC in PAs, particularly in developing countries, have advantages for sustaining the global biodiversity and their multifold ecological and socioeconomic benefits.

Like other countries, with the major objective of protecting biodiversity-enriched sites from human pressures and preserving endangered and endemic species, Ethiopia has gazetted different PAs, including 20 national parks, since the late 1960s (Temesgen et al., 2022). PAs in Ethiopia are known for their biodiversity, ecological services, opportunities for ecotourism development and livelihood sources, particularly for local communities (Mekonnen, 2022). Nevertheless, unregulated and ecologically destructive socioeconomic pressures from people living in PAs and surrounding areas resulted in rapid LUC processes, habitat impoverishment, and biodiversity loss in most of Ethiopia's PAs (Temesgen et al., 2022; Tesfaw et al., 2018). Studies have indicated that due to the bulging out of the number and density of human and livestock population, land conversion to human uses and degradation have been perpetuating rampantly, with looming loss of PAs' functionality, including NNP (where this study was conducted) (Menbere, 2021). Overall, due to the rapidly growing and diversifying anthropogenic activities, most of the PAs in the country are currently on the edge of collapse with a drastic extinction of their flora and fauna species, including large wild animals (Muhammed et al., 2016; Tesfaw et al., 2018).

Among the gazetted PAs in Ethiopia, NNP is the richest in biodiversity (flora and fauna) within highly diversified ecosystems that range from evergreen forests to aquatic ones (Mekonnen, 2022). It is also known globally for its multifold ecological services. In addition, NNP has played a prominent role in maintaining the livelihoods of many rural and urban dwellers for a long time (Fetene et al., 2015). However, similar to other PAs in Ethiopia, due to the rise of anthropogenic activities: expansion of cultivated and settlement areas, exhaustive livestock grazing, and overproduction of wood for fuel and other uses, NNP has been exposed to rampant LUC and degradation (Deribew, 2019; Mekonnen, 2022). The recurrence of wildfires and encroachment of invasive shrubs and bushes are other escalating factors of the LUC dynamics and other ecological problems. As a result, it is currently identified as one of Ethiopia's PAs that are strained by serious habitat, biodiversity, and species losses, including endemic and rare ones (Mekonnen, 20220; Muhammed et al., 2016).

Empirical and precisely measured evidence about FLUC, particularly in areas where preserved for biodiversity conservation and protection, but under pressures of degradation, and human interventions is vital for better understanding the spatiotemporal trends of the change, examining its adverse consequences on biodiversity and ecosystem services, and designing feasible and proactive strategies that enable to monitor the expected changes and their consequences with minimal cost of interventions (Cunha et al., 2021). However, in Ethiopia, the attention given for quantifying and mapping the FLUC trends of PAs is very scant, specifically for NNP has not yet been predicted and mapped.

Remote Sensing data (Satellite imageries) and Geographic Information System (GIS) tools are essential for quantifying and mapping the spatiotemporal changes in land use and cover (Cunha et al., 2021). There are also different statistical and spatial models for simulating and predicting FLUC (Legesse, 2019). However, the key challenge is lack of/ identifying/ a model that can simulate and forecast FLUC with consideration of the spatiotemporal variations in magnitude and drivers of the change (Zadbagher et al., 2018). Among the available land change prediction models, the Cellular Automata-Markov chain model (CA-Markov) is the most commonly recommended and used model because of its capability for simulating and predicting FLUC by taking into account both the spatial and temporal dimensions of multidirectional land transition processes (Hyandye & Martz, 2017).

Moreover, a comprehensive measurement and information regarding the transitions' nature and intensity in LUC are valuable for better understanding, informed decisions, and enhanced management (Aldwaik & Pontius, 2012). In this regard, integrating the CA-Markov model with appropriate change analysis tools is crucial. Among the land change analysis models /methods/, Intensity Analysis is the most comprehensive mathematical method that enables us to examine the intensity of LUC characteristics simultaneously at the interval, category, and transition levels. It is also useful to generate information about stationarity, uniformity, and the reasons behind each transition (Aldwaik & Pontius, 2012).

Therefore, this study was conducted at NNP in the Southern part of Ethiopian Rift Valley Lake Basin (ERVLB) to predict and analyze the intensities of FLUC within the time intervals: 2020-2040 (First Time Interval of Prediction; FTIP) and 2040 -2060 (Second Time Interval of Prediction; STIP) by using the CA-Markov model and intensity analysis framework. The results obtained from such a detailed study can be helpful to managers, planners, and other stakeholders of NNP to have clear evidence concerning the FLUC characteristics such as fast/slow, active/dormant, and targeted/avoided; to identify stationary trends and systematically targeted transitions and then to implement economically reasonable and ecologically targeted future management plans. Additionally, the study's results can be input to quantify the effects of FLUC on biodiversity and ecosystem services in the study area.

## MATERIALS AND METHODS

### Study Area

The study site is found between 5°51' and 6°05' N latitude, and 37°32' and 37°48' E longitude (Fig. 1) with a 41400ha area coverage. It is located at East of Arba Minch Town, in the upper part of Segen river catchment of ERVLB. The meteorological data collected from the Ethiopian Meteorology Agency (EMA, 2022) showed that in the study area, the total annual Rainfall is between 622 and 1177 mm, with 888.38mm average value for 33 years. The average annual minimum and maximum temperatures are between 16 and 20$^0$C, and 30 and 35$^0$C, respectively.

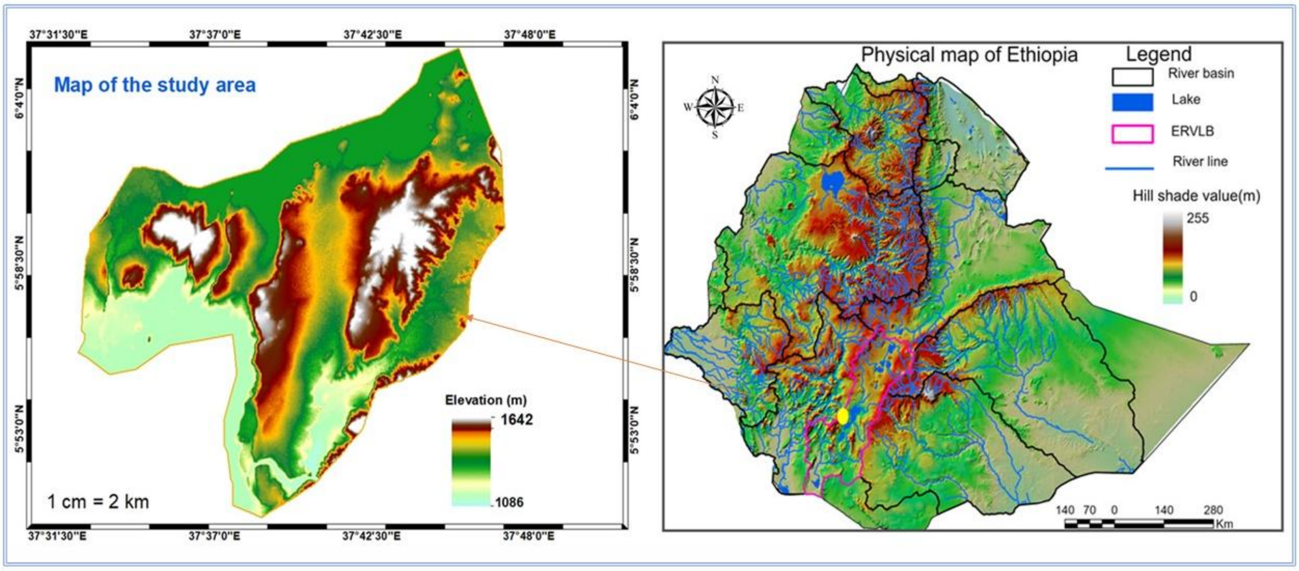


**Figure 1**

Map of the study area **(Note:** this study area map was adopted from (Mekonnen, 2022; Tadesse, 2020; Tsegaye et al., 2017) and used merely for research purposes)

NNP is one of the most important natural heritages for biodiversity conservation in Ethiopia, containing more than 90 mammal, 350 bird, and 800-1000 plant species with a significant number of endemic and endangered species (Muhammed et al., 2016). It also has a prominent role in hosting many international and continental migratory bird species. The terrestrial parts of the park covered by evergreen natural riverine forests at the Western and

Eastern edges; woodland, and bush/shrub on the volcanic hill (locally named **'God's Bridge'**), and grassland located at the Eastern part (Deribew, 2019).

The well-diversified ecosystems, natural springs, and wildlife of the park, jointly with spectacular landscapes, provide a huge opportunity for tourism development and related economic activities for Arba Minch town and the surrounding areas. Furthermore, it has been used as the main source of livelihood, income and wood demand for many semi/pastoralists/ and urban dwellers (Deribew, 2019). However, over the last few decades, due to population growth, the anthropogenic interventions for socioeconomic demands have been increased and become beyond the park's carrying capacity, leading to marked ecosystem, biodiversity and species destruction. These situations undermine the park's functionality for future biodiversity conservation and ecosystem services (Mekonnen, 2022). Thus, examining the trends and intensity of FLUC is imperative to understand the potential impacts of the changes and to address them by implementing evidence-based and long-term management plans.

### Image Acquisition, Preparation and Classification

In this study, Landsat images of 1986, 2002, and 2020 were downloaded from the United States Geological Survey /USGS/ (http://glovis.usgs.gov) to generate data about historical land use change trends that were used as input for simulating and predicting FLUC. All the images were already projected to UTM projection, zone 37, and WGS 84 datum. To minimize the cloud effect, they were taken from the dry seasons with cloud cover (0%). The necessary image preprocessing activities, Geometric and Atmospheric corrections, were processed in ERDAS Imagine 2015. The preprocessed images were classified into six land use types: forest, woodland, bush/shrubland, grassland, water area, and cultivated land in ArcGIS 10.8 using the Support Vector Machine algorithm (Franc et al., 2011; Medina et al., 2019). The detailed description and nomenclature of land types are presented in Table 1.

**Table 1**

Nomenclature and descriptions of land use types: Adopted from (Fetene et al., 2015)

| Land type | Descriptions |
|---|---|
| FL | Includes natural forests along river courses with a tree canopy of more than 10% |
| BS | Areas covered by the mixture of small shrubs and bushes with a range of 2 to 5m height |
| WL | Includes areas covered by dense woodland with trees' height range from 6 up to 20 m, and open woodland (Wooded grassland), which dominated by grasses and herbs |
| GL | Includes areas covered by grasses that are used for wild animals and livestock grazing |
| WA | The part of the park that is covered by water (rivers and parts of lakes) |
| CL | It includes all areas used for crop production and rural houses inside the park. |

***** FL= Forest, BS= Bush/shrubland, WL= Woodland, GL= Grassland, WA= Water Area, and CL= Cultivated land

### Accuracy Assessment

Accuracy assessment (AC) has been considered as one of the crucial steps in land change studies for validating the accuracy level of classified images (Congalton & Green, 2008). Table 2 displays the sample size used for AC, which was determined by following the mathematical equations and the rule of thumb specified by (Congalton & Green, 2008). The training points and ground references, utilized for image classification and AC for 2020, were collected through field observations using GARMIN-GPS, whereas Topographic map (1:50,000) of the study area for 1986 and Google Earth (https://www.google.com/earth/), 2002 were used.

**Table 2**

Sample size for accuracy assessment of land use maps of 1986, 2002, and 2020

| | Land Type | *FL | BS | WL | GL | WA | *CL | Total sample |
|---|---|---|---|---|---|---|---|---|
| Year | 1986 | 50 | 86 | 252 | 112 | 128 | 50 | 678 |
| | 2002 | 50 | 123 | 241 | 84 | 128 | 50 | 676 |
| | 2020 | 50 | 211 | 133 | 78 | 139 | 50 | 661 |

*The calculated sample size of forest and cultivated land was less than 50. Thus, considering the rule of thumb in (Congalton & Green, 2008), the sample size for these land types was raised to 50

The Kappa coefficient was employed for AC, and the outputs were 90.84%, 93.52%, and 95.20% for 1986, 2002, and 2020, respectively. These results indicated that the classified land use maps are enough for post-classification operations, including FLUC prediction (Table 3).

**Table 3**

Confusion matrix results for accuracy assessment (all values in %)

| Land use type | | | FL | SB | WL | GL | WA | CL | OA | Khat |
|---|---|---|---|---|---|---|---|---|---|---|
| Year | 1986 | PA | 89.58 | 84.27 | 95.14 | 88.33 | 100 | 93.75 | | |
| | | UA | 86.00 | 87.21 | 93.25 | 94.64 | 98.44 | 90.00 | 92.92 | 90.84 |
| | 2002 | PA | 95.56 | 95.08 | 93.88 | 87.78 | 100 | 100 | | |
| | | UA | 86.00 | 94.31 | 95.44 | 94.05 | 100 | 92.00 | 94.97 | 93.52 |
| | 2020 | PA | 95.92 | 98.54 | 91.55 | 92.31 | 100 | 95.83 | | |
| | | UA | 94.00 | 95.73 | 97.74 | 92.31 | 100 | 92.00 | 96.22 | 95.2 |

PA= Producers' Accuracy; UA= Users' Accuracy; OA= Overall Accuracy and Khat = Kappa coefficient

## Data Set and Methods to Predict FLUC

The CA-Markov model was employed to simulate and forecast the FLUC in NNP by using TerrSet IDRISI software (version 20). For simulating and predicting future land use and land cover change through this model, three major steps are needed, which are discussed below in detail. Figure 3 shows the procedures and steps followed to predict the FLUC in this study.

### Preparation of Transition Probability Matrix

The Markov Chain (MC) was used to quantify the probability rate of transitions among different land use types between two points of a given time interval. It is the most widely used and effective model (Gidey et al., 2017; Liping et al., 2018; Shaar et al., 2021). I.e., MC helps us to produce the transition probability matrixes and transition areas from historical land use maps. The distribution of each land use type at time t+1 (Lt+1) projection is determined by the distribution of land types at time t (Lt) and transition probabilities, calculated by (Equation 1) (Waseem et al., 2015). The transition probability matrix ($P_{ij}$) from $i^{th}$ land type to $j^{th}$ type was computed based on the matrix (Equation 2).

$$L_{+1} = P_{ij} * L_t \quad (1)$$

$$Pij = \begin{matrix} P11 & P12 & \cdots & P1n \\ P21 & P22 & \cdots & P2n \\ \vdots & \vdots & \vdots & \vdots \\ \vdots & \vdots & \vdots & \vdots \\ Pn1 & Pn2 & \cdots & Pnn \end{matrix} \qquad (2)$$

$$* \left(0 \leq P_{ij} \leq 1 \text{ and } \sum_{j=1}^{n} Pij = 1, (i, j = 1, 2, 3, \dots, n)\right) \qquad (3)$$

Where; $L_t$ and $L_{t+1}$ are the status of land use types at time t and time t+1, respectively; $i^{th}$ land use type at time t and $j^{th}$ land type at time t+1 and n is number of land types in the study area.

### Preparation of Suitability Maps

The suitability maps indicate the suitability level of each pixel for transferring from a land use type to other types. They can be prepared by generating information from socioeconomic and biophysical factors /explanatory variables/ (Zadbagher et al., 2018). In this study, seven static variables were initially identified based on empirical literature (Gashaw et al., 2018; Gidey et al., 2017; Legesse, 2019; Tadese et al., 2021) and the researchers' lived experience in the study area. Among these, distance from cultivated, roads, water bodies, and slope of the study area, which had relatively higher predictive power, were considered to produce suitability maps by using the Support Vector Machine algorithm with the Kernel of RFB in TerrSet (Fig. 2).

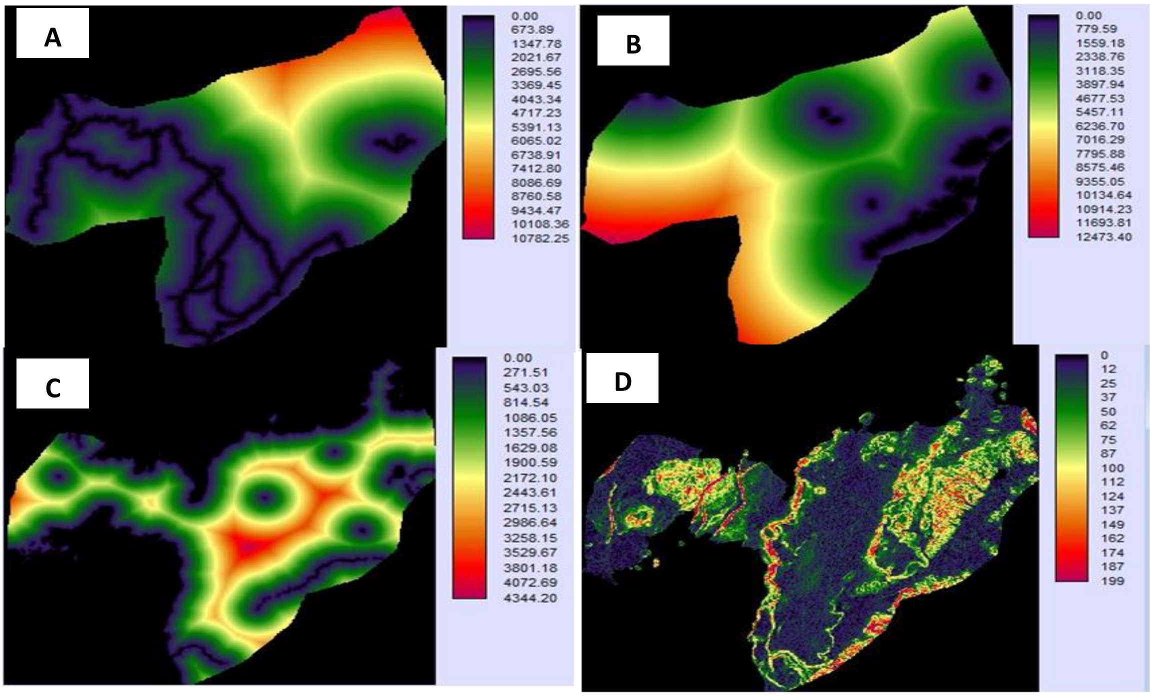


**Figure 2**

Maps of explanatory variables: **(A)** distance from roads, **(B)** distance from cultivated areas, **(C)** distance from Water bodies, and **(D)** slope in the study area

The Cellular Automata (CA) model (Equation 4) is more effective for simulating and predicting FLUC with adequate consideration of the spatial dimension of change at the expense /little/ consideration of the temporal aspects. On the contrary, the MC is more effective for considering the temporal dimensions of change (Shaar et al., 2021). Since the CA-Markov model contains the advantages of both CA and MC models, opted to predict FLUC in NNP.

$$(t, t+1) = f(S(t), N) \qquad (4)$$

Where, $f$ is the transformation rule of cellular states in local space, N is the Cellular field, and S is the set of limited and discrete cellular states

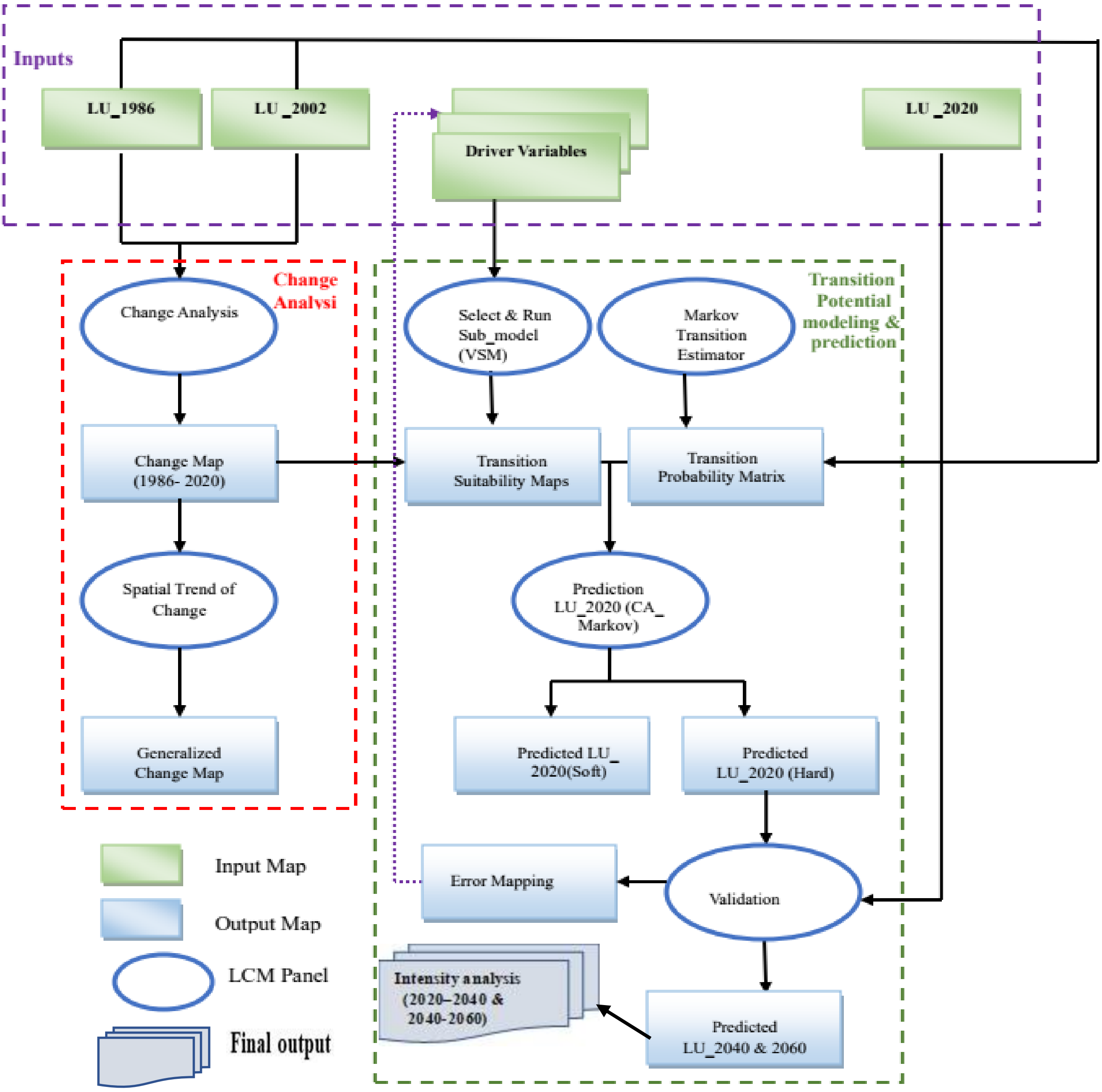


**Figure 3**

Flow chart of the procedures and steps for predicting FLUC in the study area

**Model Validation Techniques**

Model validation is one of the preconditions for effective prediction of future land use and land cover change trends and patterns (Shaar et al., 2021**).** In this study, the prediction performanceof CA-Markovwas checked by using the Kappa Index of Agreement/Disagreement (KIA) in TerrSet. KIA is the most commonly used statistical technique (Gidey et al., 2017; Liping et al., 2018; Shaar et al., 2021). If the values of KIA statistics are between 0.60 and 0.8, it indicates the model is sufficient, and greater than 0.80, it is highly sufficient for predicting the trends and patterns of FLUC (Shaar et al., 2021). In this study, model validation processes were undertaken by simulating and predicting the land use patterns of 2020 based on the transition probabilities obtained from the land use maps of 1986 and 2002. Additionally, area and visual comparisons between the actual and predicted use maps of 2020 for each land use type were also made for further validation of the model's performance. After the validation processes were completed, the CA-Markov was applied to predict FLUC for 2040 and 2060 by using the transition probabilities generated from the land use maps of 1986 and 2020 and 2020 and 2040, respectively.

**Intensity Analysis (IA)**

The transition matrix was primarily used to compute the pixel counts of persistence land, and gross gains/losses for each land use type during the FTIP (2020 - 2040) and STIP (2040 - 2060). Although helpful for interpreting some characteristics of LUC, the output of the transition matrix is not enough to distinguish whether the observed transitions are due to the area proportion of each land use type or the strength/intensity/ of the change (Aldwaik & Pontius, 2012). Thus, further analysis with consideration of the effects of the spatial extent of each land use type, strength of transition/gain and loss/, and duration of time intervals, is necessary to get sufficient and reliable information. Accordingly, the Intensity Analysis framework (IA) was applied to examine the intensity of FLUC in both time intervals of the prediction. IA is important to quantify the underlying characteristics of land use and land cover change at three levels: interval, category, and transition, and to identify the stationary and uniform patterns (Aldwaik & Pontius, 2012). The procedures of the IA model are displayed (Fig. 4).

The Interval level of intensity analysis (ILI) is the $1^{st}$ level of IA that was applied for computing the size of FLUC and the annual rate of change across each time interval (Equation 5). It is important to answer the question, in which time intervals is the annual rate of overall change relatively slow versus fast (Aldwaik & Pontius, 2012). The IA at this level compares the observed annual change intensity with a uniform intensity that would exist if the annual changes were uniformly distributed across the entire time interval, which is calculated based on (Equation 6) (Aldwaik & Pontius, 2012).

The category level of intensity analysis (CLI) is the $2^{nd}$ level of IA and used to analyze the intensity of gross gain and loss across the land use types and identify which land use types are relatively dormant versus active in terms of both annual gain and loss within a given time interval. The intensity of annual gain and loss was calculated by (Equations 7 and 8), respectively.

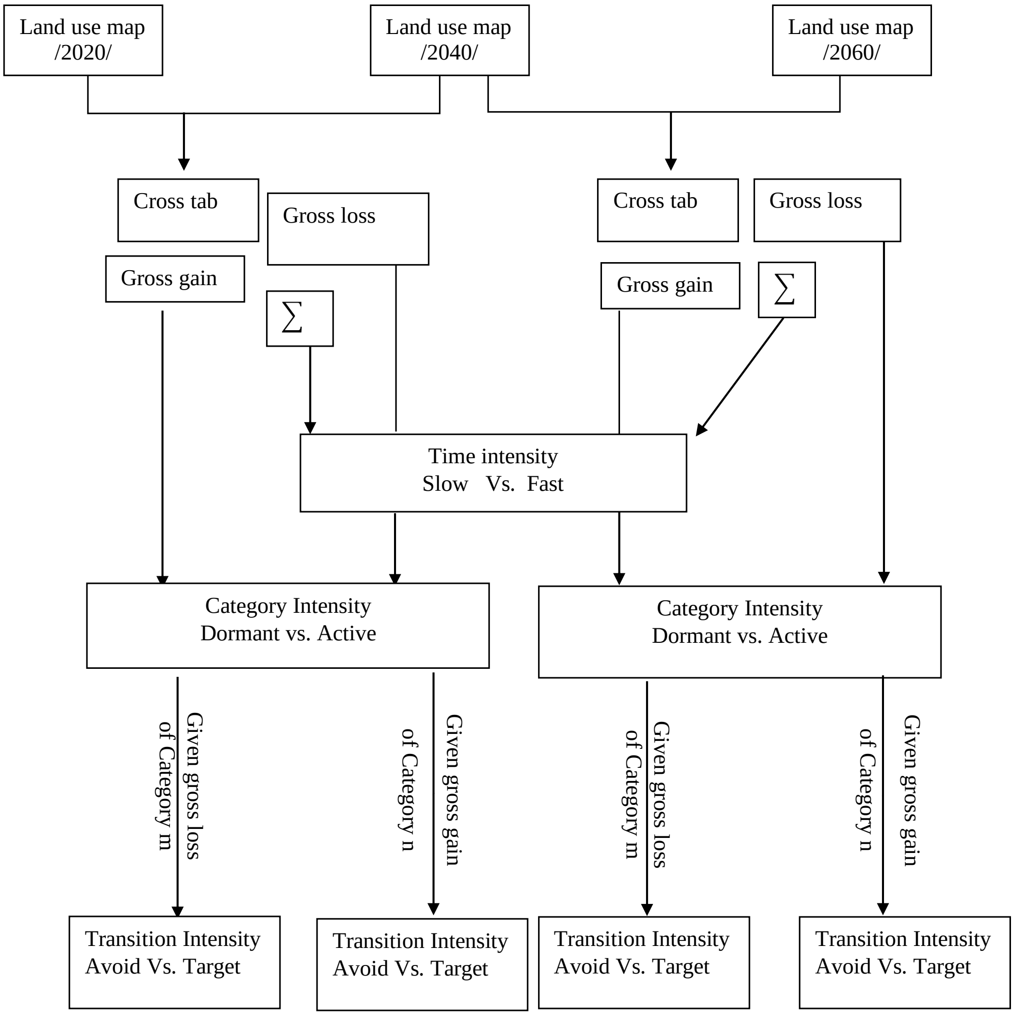


**Figure 4**

Flow chart of intensity analysis (Aldwaik & Pontius, 2012)

The 3rd level of IA is the transition level of intensity analysis (TLI), and applied to quantify the intensity of transitions among land use types. It enable us to identify transitions that are systematically targeted and avoided (Aldwaik & Pontius, 2012). Equation (9) was used to calculate the intensity of the transition from type i to n during the interval [Yt, Yt + 1], where I # n. Equation (10) was applied to calculate the uniform intensity of the transitions from all non-n types to type n (Yt, Yt + 1). If $R_{tin}$ is greater than $W_{tn}$, then the gain in n displaces i; if $R_{tin}$ is less than $W_{tn}$, then the gain in n does not affect i (Aldwaik & Pontius, 2012). Likewise, the losing component of TLI is employed to quantify the size of land transitions from the losing land types. Equation (11) computed the observed intensity of the transition from land use type m to type j during the given time interval (Yt, Yt + 1) relative to the size of type j at time t+1, where j # m and equation (12) used for the uniform intensity of transition from land type m to all other non-m types (Yt, Yt+1) relative to the size of all non-m types at time t+1. If $Q_{tmj}$ is greater than $V_{tm}$, then j targets the loss in m; if $Q_{tmj}$ is less than $V_{tm}$, then j avoids the loss in m (Aldwaik & Pontius, 2012). Table 4 shows the mathematical symbols and notations of IA, adopted from (Aldwaik & Pontius, 2012).

$$St = \frac{\sum_{j=1}^{J} \left[\left(\sum_{i=1}^{J} C_{tij}\right) - C_{tij}\right] / \left[\sum_{j=1}^{J} \left(\sum_{i=1}^{J} C_{tij}\right)\right]}{Y_{t+1} - Y_t} x100\% \tag{5}$$

$$U = \frac{\sum_{t=1}^{T-1} \left\{\sum_{j=1}^{J}\left[\left(\sum_{j=1}^{J} C_{tij}\right) - C_{tij}\right]\right\} / \left[\sum_{j=1}^{J}\left(\sum_{i=1}^{J} C_{tij}\right)\right]}{Y_T - Y_1} \text{x}100 \tag{6}$$

$$G_{tj} = \frac{\left[\left(\sum_{i=1}^{J} C_{tij}\right) - C_{tij}\right] / (Y_{t+1} - Y_t)}{\sum_{i=1}^{J} C_{tij}} \text{x}100 \tag{7}$$

$$L_{ti} = \frac{\left[\left(\sum_{j=1}^{J} C_{tij}\right) - C_{tij}\right] / (Y_{t+1} - Y_t)}{\sum_{j=1}^{J} C_{tij}} \text{x}100 \tag{8}$$

$$R_{tin} = \frac{C_{tin} / (Y_{t+1} - Y_t)}{\sum_{j=1}^{J} C_{tij}} \text{x}100 \tag{9}$$

$$W_{tn} = \frac{\left[\left(\sum_{i=1}^{J} C_{tin}\right) - C_{tnn}\right] / (Y_{t+1} - Y_t)}{\sum_{j=1}^{J} \left[\left(\sum_{i=1}^{J} C_{tij}\right) - C_{tnj}\right]} \text{x}100 \tag{10}$$

$$Q_{tmj} = \frac{\left[C_{tmj} / (Yt+1-Yt)\right]}{\sum_{i=1}^{J} C_{tij}} x100 \tag{11}$$

$$V_{tm} = \frac{\left[\left(\sum_{j=1}^{J} C_{tmj}\right) - C_{tmm}\right] / (Yt+1-Yt)}{\sum_{j=1}^{J} \left[\left(\sum_{i=1}^{J} C_{tij}\right) - C_{tim}\right]} x100 \tag{12}$$

**Table 4**

Mathematical symbols and notations of variables used in intensity analysis

| Symbols | Meaning of Symbols |
|---|---|
| J | Number of land types |
| j | Index for a type at the final time point for a particular time interval |
| i | Index for a type at the initial time point for a particular time interval |
| T | Number of time points |
| m | Losing type index for the selected transition |
| n | Gaining type index for selected transition |
| t | Index for the initial time point of interval [Yt, Yt+1], where t ranges from 1 to T-1 |
| $Y_t$ | Year at time point t |
| $C_{tij}$ | Number of pixels that transition from type i at time Yt to type j at the time Yt+1 |
| St | Annual change for time interval [Yt, Yt+1] |
| U | Value of uniform line for time intensity analysis |
| $G_{tj}$ | Annual intensity of gross gain of type j for time interval [Yt, Yt+1] relative to the size of type j at time t + 1 |
| $L_{ti}$ | Annual intensity of the gross loss of type i for time interval [Yt, Yt+1] relative to the size of type i at time t |
| $R_{tin}$ | Annual intensity of transition from type i to type n during the time interval [Yt, Yt+1]; where I # n |
| $W_{tn}$ | Value of uniform intensity of transition to type n from all non-n types at time Yt during time interval [Yt, Yt+1] |
| $Q_{tmj}$ | Annual intensity of transition from types m to type j during the time interval [Yt, Yt+1]; where j # m |
| $V_{tm}$ | Uniform intensity of transition from type m to all non-m types at time Yt+1 during time interval [Yt, Yt+1] |

## RESULTS AND DISCUSSIONS

### Magnitude and Trends of LUC from 1986 to 2020

The results of the historical LUC analysis in Table 5 indicated that all land use types in the study area experienced significant change, although the values differed between 1986 and 2002 and 2002 and 2020. Among the land use types, woodland had the largest (39.24 and 38.25%) share of the total land of the study area, while cultivated land accounted for the smallest (1.17% and 2.00%) in 1986 and 2002, respectively. However, in 2020, bush/shrubland covered the largest portion (34.85%) of the study area with 147% of land gain between 1986 and 2020. The woodland lowered to the third position with a 43.35% loss from its area coverage in 1986. Similarly, the proportion shared by grassland and forest declined from 17.70% and 7.73% in 1986 to 12.95% and 4.28% in 2020, respectively.

Regarding the change in spatial extent, bush/shrubland, water, and cultivated exhibited a continued expansion at the expense of other land use types. For example, a 5831ha area of bush/shrubland in 1986 was expanded by 40.43% and 76.08%, while a 16247ha area of woodland was shrunk down by 2.53% and 41.88% in 2002 and 2020, respectively. The forest and grassland coverage declined by 20.57% and 24.04% in 2002 and 30.25% and 3.66% in 2020, respectively. Although the study area is a biodiversity conservation and protection site, the analysis revealed the expansion of cultivated land by 70.15% in 2002 and 33.08% in 2020.

**Table 5**

Trends of past land use change (1986 - 2020)

| Land | Area in ha | | | Area changes in ha | | |
|---|---|---|---|---|---|---|
| type | 1986 | 2002 | 2020 | 1986 - 2002 | 2002 - 2020 | 1986 -2020 |
| FL | 3198 | 2540 | 1772 | -658 | -768 | -1426 |
| BS | 5831 | 8188 | 14418 | 2358 | 6229 | 8587 |
| WL | 16247 | 15836 | 9204 | -411 | -6632 | -7043 |
| GL | 7327 | 5566 | 5362 | -1761 | -204 | -1965 |
| WA | 8311 | 8443 | 9544 | 132 | 1101 | 1233 |
| CL | 486 | 827 | 1101 | 341 | 274 | 615 |
| Total | 41400 | | | | | |

*The sign (-) decrease in area coverage (loss)

Overall, our analysis indicated that throughout the study period, the forest, woodland and grassland remained in the losing category, whereas the rest types were in the gaining category. In line with our finding, the previous studies in different PAs of Ethiopia found a significant loss in vegetation land types due to deforestation, overgrazing, and agricultural land expansion by the local communities. For example, a study by (Debebe et al., 2023) in Semien Mountain National Park found a 366% and 159% extension in cultivated and built-up areas at the cost of 31% and 16% forest and grassland decline, respectively, from 1984 to 2020. The study by (Hailu et al., 2018) in Gibe Sheleko National Park also reported an increment trend in bush and shrubland by 51.5% and decline in forest land by 66.8%. Moreover, several land change studies conducted in non-protected areas of Ethiopia (Legesse, 2019; Shiferaw et al., 2019;Yesuph & Dagnew, 2019) have found the spatial expansion of bush and shrubland by displacing a significant portion of forest, woodland, and grassland. Concerning the cultivated land, consistent with the findings of this study, agricultural land expansion at the cost of more than 3 million $km^2$ vegetation cover of PAs was reported in USA (Lu et al., 2018). Likewise, many researchers (Bailey et al., 2015; Silva et al., 2021; Verburg et al., 2006) found a continued land conversion from forest and woodland to anthropogenic land uses in different biodiversity conservation areas of developing countries.

**Results of Model Validation**

The VALIDATE cross-tabulation module in TerrSet (version 20) was used to assess the performance of the CA-Markov model for predicting the FLUC for the years 2040 and 2060. The validation process was conducted based on the comparison of agreement and disagreement of counts and allocation of pixels between the simulated and actual land use maps of 2020, and the results are presented in (Table 6). The analyses displayed that the values of KIA statistics, $K_{no}$, $K_{location}$, $K_{location\ strata}$, and overall Kappa ($K_{standard}$) were equal and above 0.9 (90%). These confirmed that the simulated land use map was nearly the same as the actual land use map (Fig.5). This exemplifies that the CA-Markov model has sufficient performance to predict successfully the FLUC of the study area based on the given data. Like this study, previous studies in Ethiopia (Gidey et al., 2017; Legesse, 2019; Mathewos et al., 2022; Tadese et al., 2021) and elsewhere (Cunha et al., 2021; Nogueira et al., 2014; Waseem et al., 2015) were followed this method for CA-Markov Model validation and found KIA values that ensured the suitability of the model for forecasting future land use/cover change.

**Table 6**

Information allocation, Quantity, and Kappa index results for model validation

| Information Allocation | Information of Quantity | | |
|---|---|---|---|
| | No[n] | Medium[m] | Perfect[p] |
| Perfect[P(x)] | P(n) = 0.6263 | P(m) = 0.9864 | P(p) = 1.0000 |
| Perfect Stratum[K(x)] | K(n) = 0.6263 | K(m) = 0.9864 | K(p) = 1.0000 |
| Medium Grid[M(x)] | M(n) = 0.5719 | M(m) = 0.9247 | M(p) = 0.9177 |
| Medium Stratum[H(x)] | H(n) = 0.1429 | H(m) = 0.2943 | H(p) = 0.2944 |
| No[N(x)] | N(n) = 0.1429 | N(m) = 0.2943 | N(p) = 0.2944 |
| Agreement Chance | | | 0.1429 |
| Agreement Quantity | | | 0.1514 |
| Agreement Strata | | | 0.000 |
| Agreement Grid cell | | | 0.6304 |
| Disagree Grid cell | | | 0.0617 |
| Disagree Strata | | | 0.000 |
| Disagree Quantity | | | 0.0136 |

| Kappa Index of Agreement for the ability to predict for 2020 | |
|---|---|
| **Statistics** | **Index** |
| $K_{no}$ | 0.9121 |
| $K_{location}$ | 0.9109 |
| $K_{location\ Strata}$ | 0.9109 |
| $K_{standard}$ /Overall Kappa/ | 0.8933 |

In addition, the area comparisons between simulated and actual land use maps of 2020 for each land use type also approved the permissibility and fitness of CA-Markov with 94.78% of overall accuracy (Table 7). For example, the simulated area proportion of bush/shrubland and woodland (35.30%, and 20.28%) was equivalent to their actual area proportion (34.82% and 22.23%) with accuracy level of 98.65% and 90.80%, respectively. The lower consistency was relatively observed in forest and grassland with 84.08% and 85.25% accuracy, respectively, but they were reasonably matched and adequate indicators of the model's validity.

**Land Transition Probabilities for 2040 and 2060**

The FLUC simulation scenario development and prediction activities were done using TerrSet based on the datasets, statistical tools, and steps displayed in (Fig. 3). The transition matrix in (Table 8) presents the proportion of transition probabilities for each land use type converted to others during the FTIP and STIP. The bold values in the diagonal axis represent the probabilities of persisted land, and the off-diagonal values indicate probabilities of land transitions (gains/losses/ for each land use type.

**Table 7**

Comparison of area (ha) between the simulated and actual land use map of 2020

| Land use type | Actual area (ha) | Simulated area (ha) | Difference (ha) | Difference (%) | Accuracy (%) |
|---|---|---|---|---|---|
| FL | 1772 | 1511 | 261 | 15.92 | 84.08 |
| BS | 14418 | 14613 | 195 | 1.35 | 98.65 |
| WL | 9204 | 8395 | 809 | 9.20 | 90.80 |
| GL | 5362 | 6216 | 854 | 14.75 | 85.25 |
| WA | 9546 | 9535 | 11 | 0.11 | 99.89 |
| CL | 1101 | 1132 | 31 | 2.82 | 97.18 |
| Total | 41400 | 41400 | | | |

Overall accuracy = 94.78%

The study's results revealed that the lower persistence probability (< 59%) is anticipated in forest, woodland and grassland. Such types of vulnerability in natural forests and grassland landscapes are more likely attributed to deforestation and low regeneration capacity due to continued and exhaustive utilization for livestock grazing and wood production with little/no restoration practices (Debebe et al., 2023;Deribew, 2019; Mekonnen, 2022; Tsegaye et al., 2017). Similar to this study's findings, a lower persistence probability in forest and grassland was reported by (Cunha et al., 2021; Kodero et al., 2024; Nogueira et al., 2014).

As displayed in Table 8, among the vegetation land use types, bush/shrubland is the only one that experienced the highest persistence probability (≈ 71%) in both time intervals. This could be attributed to different factors. First, the nature of the land type, i.e., once established in a given landscape, it has a lower probability to transit towards other types within a short period and/or/ human interventions are needed to replace (Pierce et al., 2019). Second, in the study area, the larger portion of bush/shrubland is found at steep slopes and far away from human settlements. Third, economically, it is less useful and preferred by local communities, including for charcoal, fuel wood, and construction materials production. These situations increase the bush/shrubs' probability of persistence and stability in the study area.

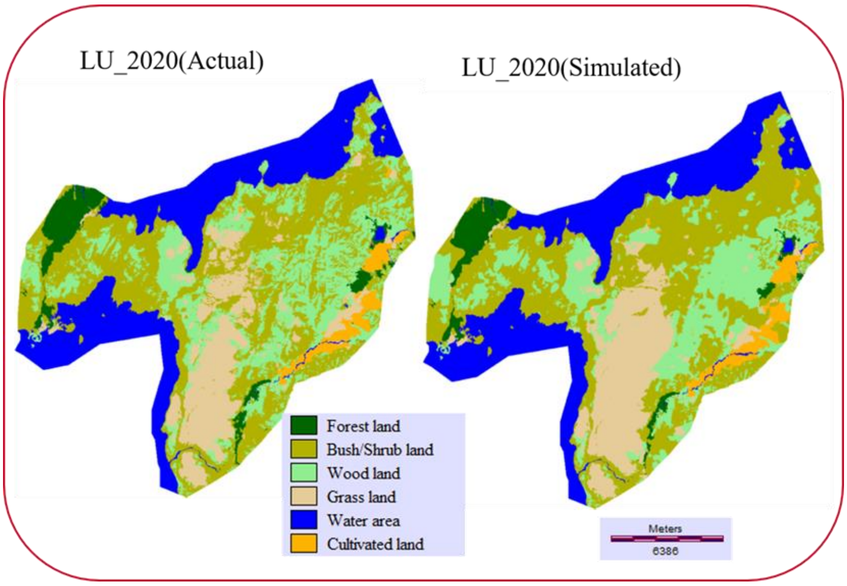


**Figure 5**
The actual and simulated land use maps of 2020

Regarding the transition probability, the study showed that the conversion to bush/shrubland from forest, woodland, and grassland attained the highest probability. The plausible reasons are the expansion of invasive shrub and bush plants, and continued degradation in the latter land use types due to continued and unsustainable utilization for livestock grazing and wood production by local communities, and by other factors (Deribew, 2019; Fetene et al., 2015; Mekonnen, 2022). Additionally, the experimental study done by (Pierce et al., 2019) found that in areas where other natural resources, such as grasslands, are under pressure from human activities and stresses from changes in abiotic factors (soil and climate), shrubs can have the opportunity to outpaceterrestrial expansionand fast regeneration. Moreover, this predicted transition probability is significantly attested by several empirical studies in Ethiopia that found the advancement of bush/shrublands in areas where forest areas and grasslands have been subjected to degradation by anthropogenic activities (Gidey et al., 2017; Legesse, 2019; Temesgen et al., 2022; Yesuph & Dagnew, 2019).

**Table 8** Land transition probability matrix for 2040 (1986 - 2020) and 2060 (2020 - 2040)

| Transition Time | | Land use type | Transition to FL | BS | WL | GL | WA | CL |
|---|---|---|---|---|---|---|---|---|
| 1986 to 2020 | Transition from | FL | **0.5532** | 0.1001 | 0.0704 | 0.0921 | 0.0673 | 0.117 |
| | | BS | 0.0347 | **0.709** | 0.1663 | 0.0125 | 0.0643 | 0.0133 |
| | | WL | 0.0043 | 0.3851 | **0.5376** | 0.0622 | 0.0067 | 0.0041 |
| | | GL | 0.0024 | 0.2349 | 0.1287 | **0.5918** | 0.0381 | 0.004 |
| | | WA | 0.0809 | 0.0505 | 0.0049 | 0.0159 | **0.8478** | 0.0000 |
| | | CL | 0.0243 | 0.0295 | 0.119 | 0.0265 | 0.022 | **0.7787** |
| 2020 to 2040 | | FL | **0.5704** | 0.1869 | 0.1345 | 0.0584 | 0.005 | 0.0447 |
| | | BS | 0.0297 | **0.7029** | 0.1901 | 0.0181 | 0.054 | 0.0051 |
| | | WL | 0.0041 | 0.5065 | **0.4363** | 0.0411 | 0.0037 | 0.0083 |
| | | GL | 0.0094 | 0.3887 | 0.1653 | **0.4128** | 0.006 | 0.0178 |
| | | WA | 0.0103 | 0.0515 | 0.0334 | 0.016 | **0.8465** | 0.0423 |
| | | CL | 0.0000 | 0.0669 | 0.0484 | 0.0339 | 0.0409 | **0.8099** |

For the transition potential to grassland, the higher value is contributed from forest and woodland. Likewise, it has also been predicted in the Western USA, from 58% of future loss transition probability in forest land, 40% will shift to grassland (Kodero et al., 2024). In normal circumstances, the direct transitions from forests to grasslands are uncommon. Similarly, transitions from woodland to grassland are naturally rare, unless supported by anthropogenic and natural factors (Sala & Maestre, 2014). However, since the last few decades, due to the influences of human activities and natural disturbances like climate change and drought, direct transitions from forest and woodland to grassland have been predominant (Legesse, 2019). In this study area, it can be associated with the massive removal of trees because of charcoal production, repeatedly occurrences of fires by unknown reasons and the pastoralists to get additional grazing land for their livestock and land for shifting cultivation, and loss of regeneration capacity in forest and woodlands (Deribew, 2019; Tsegaye et al., 2017). Similarly, the empirical studies conducted in Semen Mountain National Park (Debebe et al., 2023) and Kafta Shiraro National Park (Temesgen et al., 2022) also found a substantial land transition directly from forest and woodland to grassland, mainly caused by wildfire occurrence and over-demanding for fuelwood production. Moreover, the transition to forest, the highest value is from bush/shrubland (≈ 71%). This type of transition is common, and can be attained by two major reasons in PAs: ecological succession and human interventions to fast regeneration and expansion of forests over the areas of other land use types (Nogueira et al., 2014). Supporting the findings of this study, several studies highlighted 5 to 30% transition probabilities to forest from shrublands as a result of ecological succession and reforestation (Bieluczyk et al., 2023; Gui et al., 2025; Nytch et al., 2023). As shown in Table 8, the highest transition to cultivated land is contributed from forest. Although it is not common naturally, this land transition probability in the study area is largely attributed to the establishment of settlements and expansion of crop land by removing the forest areas located at the Eastern edge.

**Predicted Magnitude and Trends of FLUC**

The predicted changes for each land use type were quantified based on the actual land use map of 2020 and predicted land use maps of 2040 and 2060 (see Table 9). The prediction results showed that there will be sizable land exchange among the land use types in the study area during the entire prediction period. In both time intervals, forest, woodland, and grassland are expected to exhibit considerable land loss, especially for bush/shrubland in the next four decades.

**Table 9**

Future land use change (2020 – 2060)

| Land type | Area (ha) | | | Area change (ha) | | |
|---|---|---|---|---|---|---|
| | 2020 | 2040 | 2060 | 2020 - 2040 | 2040 - 2060 | 2020 - 2060 |
| FL | 1772 | 1518 | 1438 | -254 | -80 | -334 |
| BL | 14418 | 18058 | 19551 | 3641 | 1493 | 5133 |
| WL | 9204 | 7302 | 6800 | -1902 | -502 | -2403 |
| GL | 5362 | 3176 | 1526 | -2187 | -1649 | -3836 |
| WA | 9544 | 10034 | 10660 | 490 | 626 | 1115 |
| CL | 1101 | 1313 | 1426 | 212 | 113 | 325 |
| Total | 41400 | | | | | |

*The sign (-) indicates the loss of spatial coverage (negative change)

The largest spatial expansion (35.57%) is anticipated in bush/shrubland, followed by cultivated land (29.53%) and water (11.69%), and the largest reduction is predicted in grassland (71.59%), followed by woodland (26.13%) and forest (18.85%) between 2020 and 2060. The forest, woodland, and grassland areas are expected to decline by 14%, 21%, and 41% during the FTIP, and 6%, 8%, and 52% during the STIP, respectively. Similarly, a substantial reduction in forests and grasslands in PAs was predicted by (Cunha et al., 2021; Nogueira et al., 2014). Additionally, the vast and rapid expansion of bush/shrub and agricultural land over forest lands and grasslands were projected in Ethiopia (Gashaw et al., 2018; Gidey et al., 2017; Legesse, 2019; Tadese et al., 2021), Ghana (Aniah et al., 2023), and Egypt (Nogueira et al., 2014).

**Predicted Gross Gain, Loss and Persistence Land**

The predicted land use maps in (Fig. 6), and the quantitative computations from cross-tabulation matrices in (Table 10) showed that although the values differed, all land use types are expected to exhibit sizable gain and loss transitions, as well as persistence land during both time intervals of the prediction. The results revealed that a 14.32%, 26.66 %, and 40.78% (in FTIP), and 18.85%, 26.11%, and 71.54% (in STIP) negative net change (loss) is expected in forest, woodland, and grassland, respectively. Conversely, a 35.6% (3641ha in FTIP and 1492ha in STIP) of positive net change (Gain) is anticipated in bush/shrubland over the study period. During the FTIP, the predicted land loss from grassland, woodland, and forest (51.43%, 48.67% and 32.89%) is higher than land gain (17.99%, 35.30%, and 21.67%), respectively, which is also true in the STIP, although pixel counts/land size/differed (Table 10).

**Table 10**

Pixel counts for persistence land on the main diagonal (underlined) and land changes in the off-main diagonal for 2020 - 2040 and 2040 -2060 (**in bold**)

| | Land use type | Final year of the time interval | | | | | | Initial total | Gross Loss | Net change | Persistence(%) |
|---|---|---|---|---|---|---|---|---|---|---|---|
| | | FL | BS | WL | GL | WA | CL | | | | |
| Initial year of the time interval | FL | 13212 | 2817 | 2028 | 881 | 76 | 674 | 19688 | 6476 | 2820 | 67.11 |
| | | **11248** | **2338** | **2953** | **60** | **90** | **179** | **16868** | **5620** | **892** | **66.68** |
| | BS | 2772 | 132479 | 17740 | 1692 | 5038 | 474 | 160195 | 27716 | 40451 | 82.70 |
| | | **4364** | **164927** | **21520** | **2750** | **6482** | **603** | **200646** | **35719** | **16583** | **82.20** |
| | WL | 362 | 44719 | 52495 | 3627 | 324 | 737 | 102264 | 49769 | 21132 | 51.33 |
| | | **336** | **36112** | **42550** | **1363** | **329** | **442** | **81132** | **38582** | **5572** | **52. 43** |
| | GL | 493 | 20283 | 8628 | 28935 | 311 | 929 | 59579 | 30644 | 24296 | 48.57 |
| | | **28** | **13850** | **8536** | **12783** | **54** | **32** | **35283** | **22500** | **18327** | **36.23** |
| | WA | 29 | 145 | 94 | 45 | 105617 | 119 | 106049 | 432 | 5441 | 99.59 |
| | | **0** | **1** | **0** | **0** | **111487** | **2** | **111490** | **3** | **6952** | **100.00** |
| | CL | 0 | 203 | 147 | 103 | 124 | 11653 | 12230 | 577 | 2356 | 95.28 |
| | | **0** | **1** | **1** | **0** | **0** | **14584** | **14586** | **2** | **1256** | **99.99** |
| Final Total | | 16868 | 200646 | 81132 | 35283 | 111490 | 14586 | | | 96496 | |
| | | **15976** | **217229** | **75560** | **16956** | **118442** | **15842** | | | **49582** | |
| Gross Gain | | 3656 | 68167 | 28637 | 6348 | 5873 | 2933 | | 115614 | | |
| | | **4728** | **52302** | **33010** | **4173** | **6955** | **1258** | | **102426** | | |

* The records for net change are in their absolute values

About persistency, the highest percentage of persisted land (above 83%) is expected in water, followed, by cultivated land and bush/shrubland (Look at the last column in Table 10), whereas the lowest (48.57% and 36.23%) is expected in grassland followed by woodland (51.33% and 52.45%) and forest (67.11% and 66.68%) during the FTIP and STIP, respectively. With slight differences, these findings are consistent with the findings of (Aniah et al., 2023; Mathewos et al., 2022; Waseem et al., 2015). The gain-loss-persistent analysis indicated that, like the historical LUC processes, the FLUC in the study area will be characterized by non-linear, multidirectional, and intensive loss of land from forest, woodland, and grasslands.

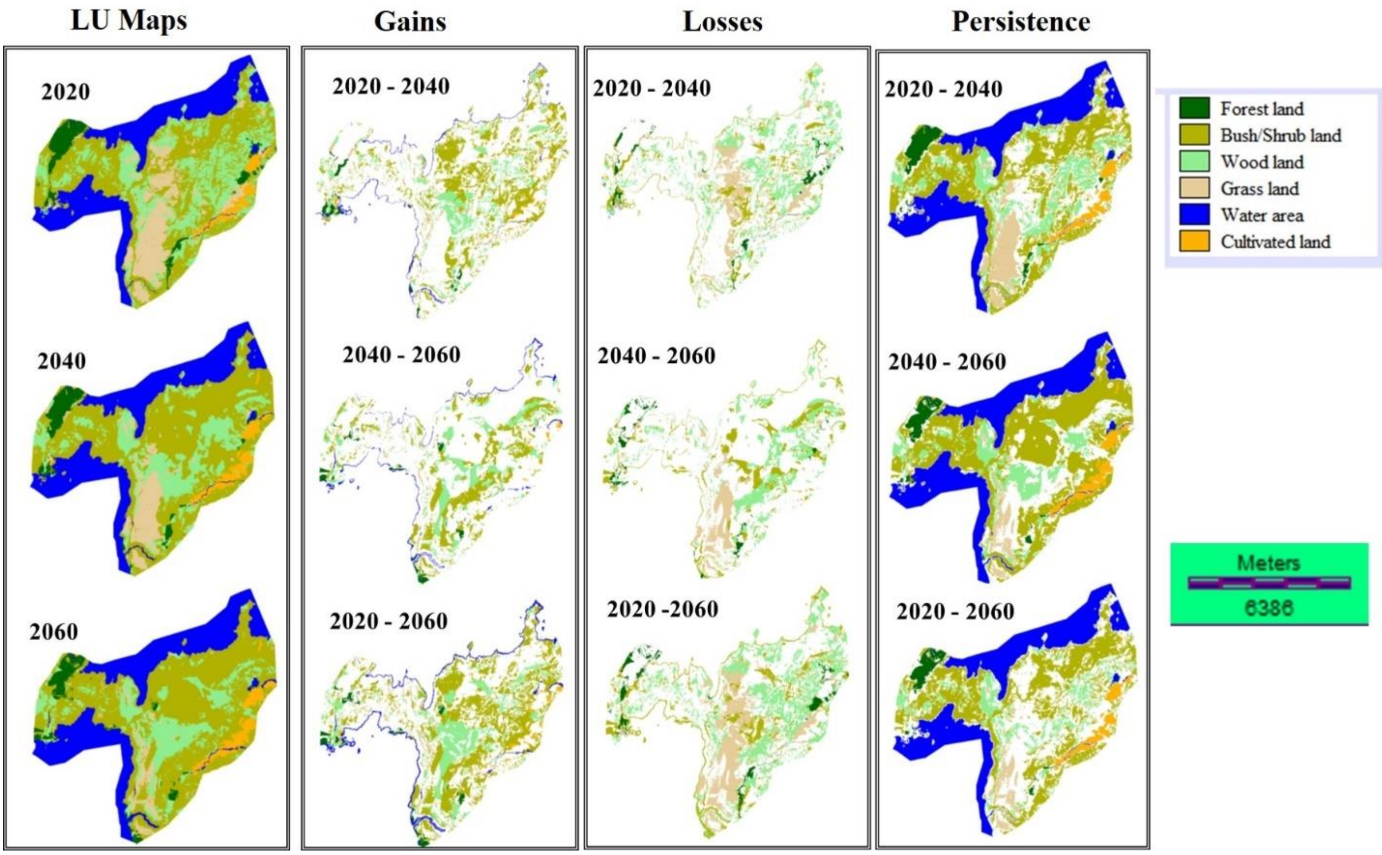


**Figure 6**

Future land use maps and changes from 2020 – 2040, 2040 – 2060 and 2020 – 2060

**Intensity of Predicted Land Use Changes (2020 – 2040 and 2040 – 2060)**

**Interval Level of Intensity Analysis (ILI)**

In Figure 7 of the ILI analysis, the left side of the graph shows the percentage of area change and the right side indicates the percentage of change intensity. The vertical broken line displays the intensity of uniform change (1.18%). The analysis demonstrated that the overall FLUC (50.27%) predicted in FTIP will be higher than STIP (44.53%). It will also prevail quickly in FTIP (1.26%) and slowly in STIP (1.11%). As shown in (Fig.7) the intensity bars are not at the uniform line, which indicates the predicted FLUC will not be uniform and perfect stationary for the ILI, and the intensiveness of the changes is more likely important than the length of time intervals for land transition during the coming four decades in NNP.

**Category Level of Intensity Analysis/CLI/**

The CLI of intensity analysis is shown in (Fig. 8). In both graphs (A&B) the paired bars on the left side show the gross annual gain and loss of each land use type. The results of the CLI displayed that the largest annual gain is predicted in bush/shrubland, whereas the largest annual loss is predicted from woodland, followed by grassland and bush/shrubland in both time intervals.

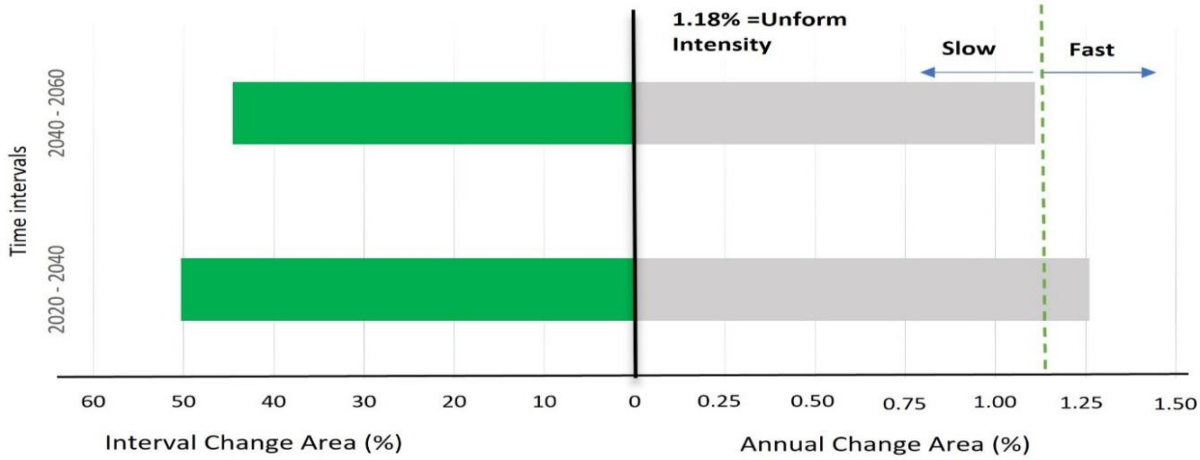


**Figure 7**
Interval level of intensity analysis for time intervals: 2020 – 2040 and 2040 – 2060

As shown in the left side of Figure 8; in the study area, land use types with smaller area coverage will experience relatively smaller size of land transitions/gains and losses/, and the land use types with the larger area coverage also exhibit relatively larger land transitions. However, the land type with the smallest size of transition, will have no the most dormant intensity and the land type with largest transition have no the most active intensity/gain and loss/, as shown on the right side of the same figure (Fig. 8). These indicate that examining the intensity of annual gain and loss transition for each land type is necessary to understand whether the transferred land size is due to the area proportion at the initial time or the strength of change (Aldwaik & Pontius, 2012). The broken vertical lines in graphs A & B of (Fig. 8) indicate the intensity of the uniform annual change, which is expected in the FTIP and STIP.

During both time intervals, the most dormant annual gain and loss transitions are predicted in water and cultivated land. while active gain and dormant loss are predicted in bush/shrubland. The results indicated that for gaining transitions of shrub/bushland, the intensiveness of the changes is more likely important than the larger area proportion at the initial time, and the opposite is true for its losing transitions. The loss intensity of grassland is expected to be the most active in both time intervals, whereas its gain is dormant and less active during FTIP and STIP, respectively. Similarly, the annual gain and loss in woodland are more likely to be active at both time intervals, while the predicted gain in forest is dormant in the FTIP but active in the STIP. The loss intensity analysis for forest revealed active loss in both time intervals and active gain in the STIP. These results indicated that the predicted gain in forest, woodland, and grassland, mainly attributed to their area proportion, whereas the losses from these land types can be significantly attributed to the intensiveness of changes, i.e., the drivers that forced the land types to lose their area. Regarding stationarity at CLI, the predicted gain and loss transitions in all land use types, except the gain in grassland and forest, are expected to be stationary, although not perfect.

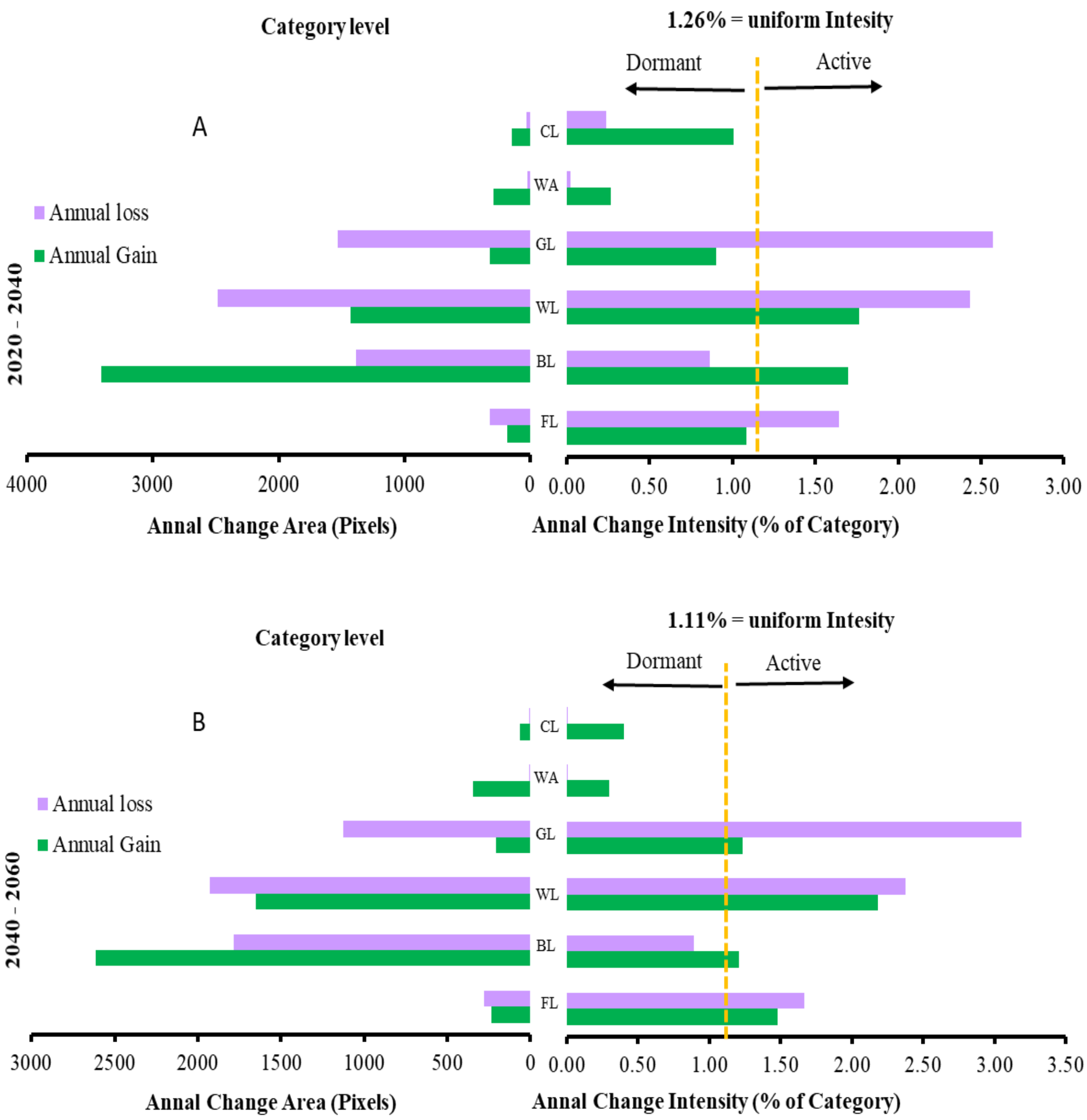


**Figure 8**

Category level of intensity analysis for 2020 - 2040 (A) and 2040 -2060 (B)

**Transition Level of Intensity Analysis (TLI)**

In the study area, forest, woodland, and grassland are the major natural resources and the most importantforbiodiversityconservation,ecologicalservices, and livelihood opportunities for people living in NNP and surrounding areas (Mekonnen, 2022). However, the land change analyses (1986 to 2060) demonstrated that these land types have been under intensive loss transitions and significantly replaced by bush/shrubland. Therefore, the TLI analysis for FLUC focused on the transitions to bush/shrubland (gains) and transition from forest, woodland, and grassland (losses).

As shown on the left side of (Fig. 9), in both time intervals, the predicted annual gain of bush/shrubland is contributed from all land use types, but the largest contribution is expected from woodland, followed by grassland and forest. However, the transition intensity on the right side revealed that the gain of this land type intensively targeted only the loss transition from woodland

and grassland and avoided others in both time intervals. As it can be seen in the graph, above 50% of the intensity bars for woodland and grassland extended to the right of the uniform lines; exemplifying the gain of bush/shrub from these land use types for the next four (4) decades more likely due to the intensiveness of the transitions/strength of drivers of the changes but rather the largeness of its area. Moreover, the TIL also indicated that all the land transitions toward bush/shrubland are expected to be stationary, even though no one is perfect.

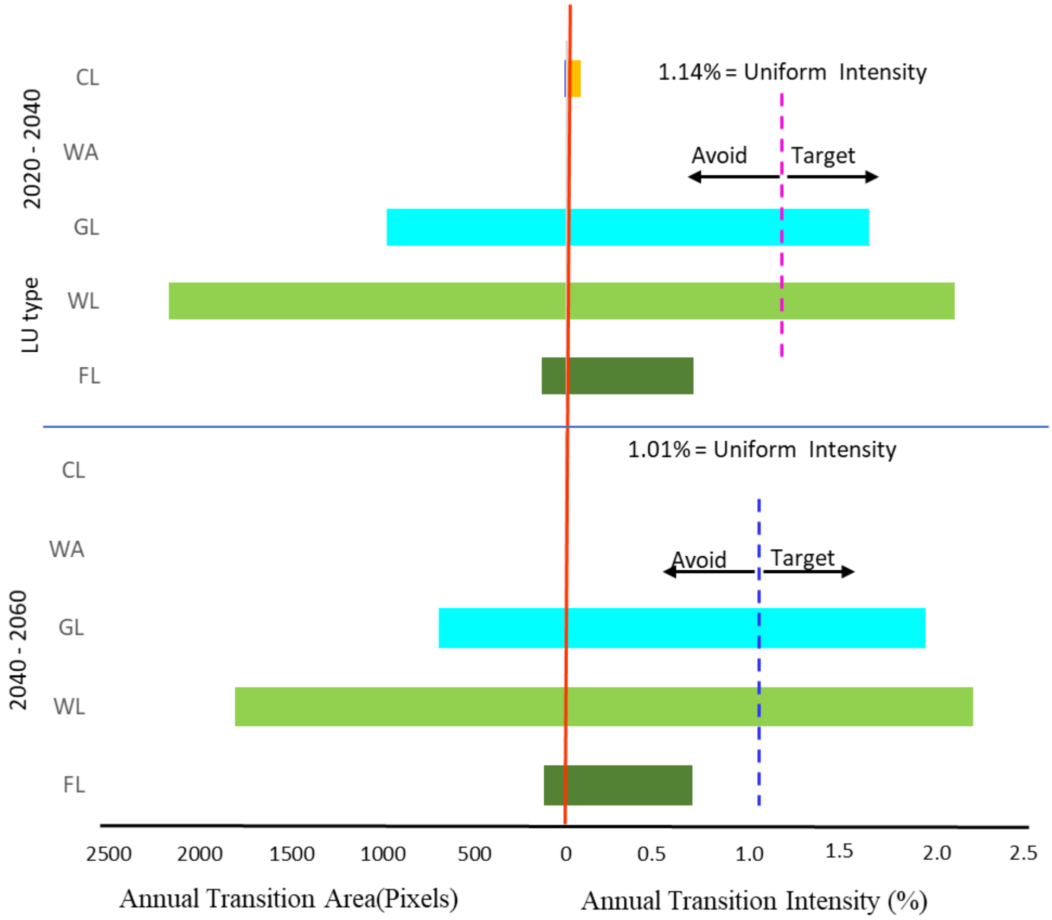


**Figure 9**

Transition intensity to Bush/shrubland (BS) during 2020-2040 and 2040 -2060

Figure 10 displays the area transition (left side) and transition intensity (right side) from forest, woodland, and grassland to other types. The results of TLI showed that the predicted land loss from forest is anticipated to be replaced by all other land use types, with the largest portion by bush/shrubland in both time intervals. However, the transition intensity on the right side of Figure 10 pointed out the predicted loss of forest is expected to be intensively targeted by cultivated land, although the strength will be relatively lower in FTIP and woodland in the STIP. Similarly, the loss from woodland will be targeted by bush/shrubland and avoided by other land types across the study time intervals. Furthermore, the loss from grassland will also be replaced by all land types, but intensively by bush/shrubland and woodland. In addition, the transitions from forest to cultivated land, woodland and water, and from woodland and grassland to other land use types are expected to be stationary at the transition level of intensity analysis.

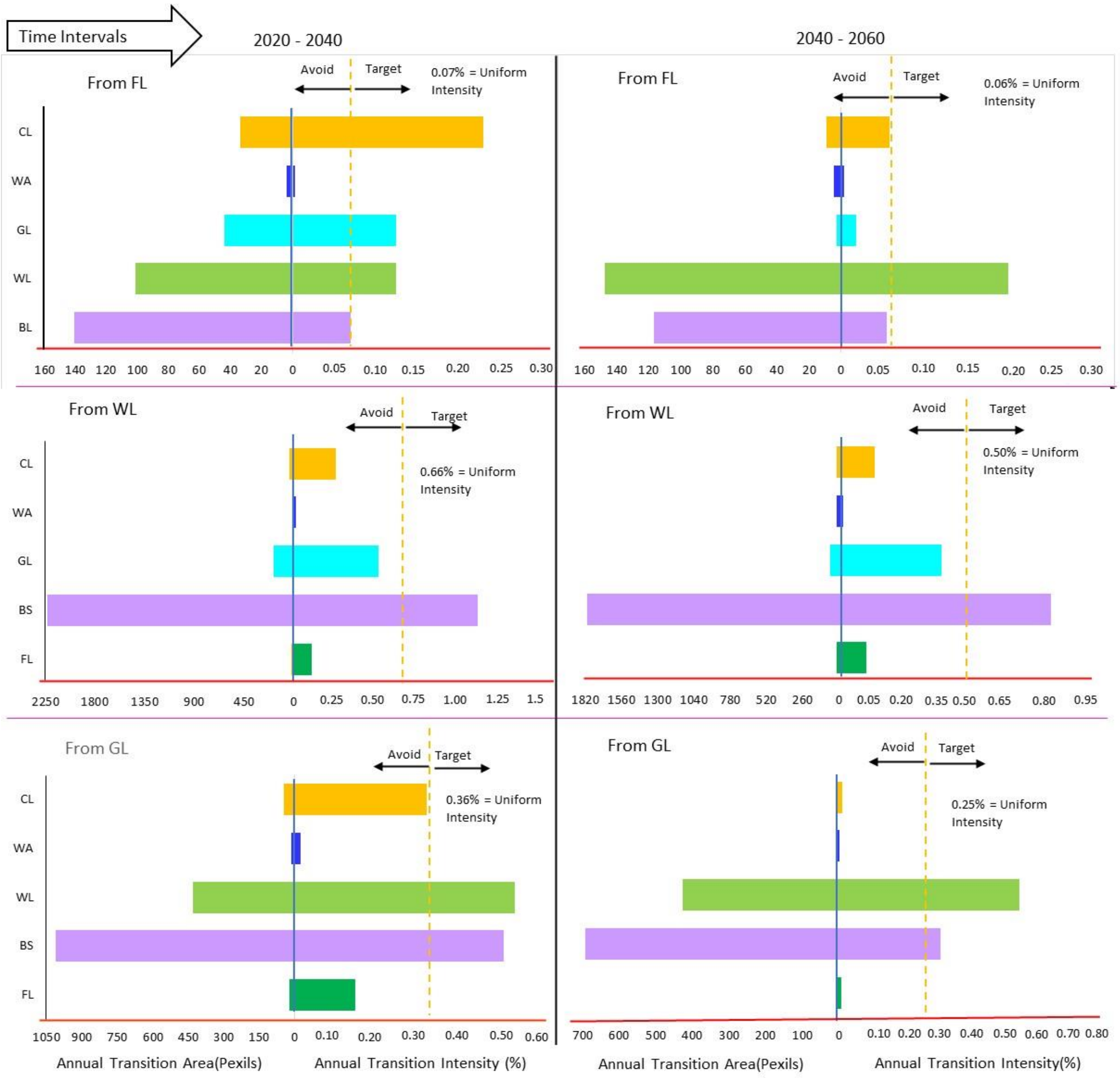


**Figure 10**
Transition intensity from forest (FL), woodland (WL) and grassland (GL) (2020-2040 &2040- 2060)

## IMPLICATIONS OF THE PREDICTED FLUC

Protected Areas (PAs) are essential for preserving biodiversity and maintaining ecosystem services (Marchese, 2015), particularly nowadays, when human activities and ecosystem destruction are rapid and worsening (Venter et al., 2016). Nevertheless, most of the PAs across the globe are suffering from the adverse consequences of human-induced land use change (LUC) and degradation (Menbere, 2021). Despite the short-term economic benefits, habitat conversion and exhaustive utilization for socioeconomic activities lead to a drastic loss of biodiversity and ecosystem services (Cunha et al., 2021; Lu et al., 2018). Eventually, it can end up with failure in PAs and long-lasting environmental and socioeconomic repercussions (Bailey et al., 2015).

The immense potential for biodiversity conservation and multiple ecosystem services of the study considerably depends on natural forest, woodland, and grassland ecosystems (Deribew, 2019; Tsegaye et al., 2017). However, the predicted land transitions for the next four decades can pose considerable threats to its future biodiversity and ecosystem services in different ways. It has been documented that due to the rise of anthropogenic encroachments, pervasive land change and degradation are the leading factors for current and future habitat and biodiversity loss in PAs, particularly in developing countries (Menbere, 2021). Apart from encompassing the largest flora diversity and a significant number of endemic plants in Ethiopia, the natural forest, woodland and grassland ecosystems in NNP are the key shelter, food and water source, and reproduction sites for fauna species, including many migratory birds Fetene et al., 2015). Thus, the anticipated active loss and dormant gain transitions in natural vegetations lead to further degradation in the remaining biodiversity of flora and fauna, through habitat impoverishment, reproduction disturbance, species loss, deterioration of regeneration capacity and so on.

Scientific studies confirmed that intensive and rapid land transitions that are mainly characterized by net loss in natural vegetation have profound impacts on ecological services of natural ecosystems (Feng et al., 2023; Kubiszewski et al., 2017; Winkler et al., 2021; Venter et al., 2016). In the study area, the Arba Minch underground water forest, Kulfo riverine forest and Sermele riverine forest, and Nechsar grassland have been known for their multitudinal ecological services, including regulation of hydrological and atmospheric processes, sequestration of GHGs, moderation of microclimate conditions, controlling of soil erosion and sedimentation, and water supply for wildlife and local communities (Fetene et al., 2015; Mekonnen, 2022). The continuous decline in forest, woodland, and grassland, and the advancement in other land types, including cultivated land, can undermine the potential of the study area for future ecological services.In addition,particularly at the local level, it can aggravate the existing environmental problems: climate change, land degradation, and shortage of water supply (Fetene et al., 2015; Mekonnen, 2022). Beyond biodiversity preservation, monitoring the ongoing LUC is crucial to maintain the ecological services of the park and to address environmental problems.

The natural resources, specifically forest and grassland in NNP, have substantial role in the livelihood and sociocultural life of local communities. For a long time, millions of farmers and urban dwellers living inside and surrounding areas highly depended on the park for their survival, job opportunities, and fuel wood demand (Deribew, 2019; Mekonnen, 2022). Additionally, the biodiversity, natural springs and other attractive natural endowments of NNP are significant contributors for the existing tourism activities and development in Arba Minch town and surrounding areas. The future degradation in these natural resources considerably affects the sustainability of the opportunities for livelihood of local communities, tourism activities, and socioeconomic development at large. Empirical studies strongly argued that the ecological problems facing biodiversity conservation sites across the globe fundamentally emanated from the lack of adequate protection by local communities for their environmental values and administrative failure to implement policies (Marchese, 2015; Menbere, 2021). Similarly, in study area, the results of LUC analyses and the researcher above 18 years lived experiences show that the continued forest and grassland degradation, bush/shrub encroachment over the entire landscape, and cultivated land expansion are the mirror of inadequate interventions for resource management and weakened enforcement of laws to control illegal economic activities. The effectiveness of ecological interventions and legal instruments may be constrained by various factors, such as using of the park area as permanent land of living by semi/pastoralists/ (Guji and Kore communities), main source of livestock grazing, fodder collection and wood production for fuel, furniture, and construction, and lack of political commitment in the local and regional governments to protect the park for biodiversity conservation (Mekonnen, 2022;Tsegaye et al., 2017). Several researchers have also documented similar problems for PAs in Ethiopia (Debebe et al., 2023; Menbere, 2021; Temesgen et al., 2022) and elsewhere (Baidoo et al., 2023). Therefore, an integrated and long-term plan is necessary for natural resource management, alternative livelihood and energy sources, and relocation of people outside the park by involving local communities, government offices, NGOs, and academic institutions to control the predicted FLUC in NNP and harness the ecological and socioeconomic advantages sustainably.

Predicting and understanding future land change has become the key concern for conservationists and land use planners because of its advantages in devising effective and alternative resource management plans (Waseem et al., 2015). In this study, the integration of CA-Markov model with intensity analysis framework provides reliable evidence for informed decisions and improved resource management plans. Additionally, quantified and mapped information about FLUC of protected areas is vital to improve public awareness and involve all stakeholders in discussions and policy-making processes (Nogueira et al., 2014; Verburg et al., 2006). In this study, although an effective change prediction model (Cunha et al., 2021; Waseem et al., 2015), and a three levels change intensity analysis tool (Aldwaik & Pontius, 2012) were applied, the prediction process was not free from limitations that generating from the errors and drawbacks in the prediction model, statistical tools that were used for data preparation, satellite images and land classification algorithm (Cunha et al., 2021; Mathewos et al., 2022; Nogueira et al., 2014; Zhang et al., 2021). Additionally, the reliability of findings regarding FLUC can be influenced by the prediction capacity of the explanatory that used in change modeling processes (Cunha et al., 2021). In this study, seven static explanatory variables were identified initially. Among the identified variables, based on their relatively higher prediction performance, distance from cultivated land, road, water bodies, and slope of the study area were used for simulating and predicting FLUC. However, the socioeconomic variables were not considered due to the absence of georeferenced and timely matched data. Therefore, we recommend future studies on this issue in this study area to take into account the dynamic environmental and socioeconomic variables.

## CONCLUSION

Due to anthropogenic pressures for socioeconomic well-being and natural drivers, NNP has been threatened by continued LUC and land degradation. Thus, detailed information about FLUC is crucial to understand the characteristics of the change and respond the adverse impacts through evidence-based proactive and targeted interventions. This study quantified the intensity of FLUC between 2020 and 2060 using the CA-Markov model and Intensity Analysis framework. The findings revealed that considerable land transition is anticipated with negative implications for biodiversity and ecological services in the coming four decades. Bush/shrubland and cultivated land will have a net gain at the expense of forest, woodland, and grasslands. Further, the analyses indicated that the predicted intensively targeted losses in forest, woodland, and grassland, and as gains in cultivated land and bush/shrubland, mainly attributed to the intensiveness of the drivers rather than the areas of the land types. Therefore, interventions, particularly for enhancing forest land, woodland, and grasslands, and controlling the expansion of bush/shrubland and cultivated land, should be implemented through the active involvement of all stakeholders and integrated management approaches. Additionally, the study highlighted the importance of integrating CA-Markov model with intensity analysis to quantify the underlying characteristics of FLUC and generate more pertinent information for informed decision and policy-making.

## ACKNOWLEDGMENTS

Our acknowledgment goes to Arba Minch University for financial and other support under grant code GOV/AMU/TH24/CSSH/GeES/05/2012. We extend special thanks to Abdulselam Turke for his language editing.

## REFERENCES

Aldwaik, S., & Pontius, R. (2012). Intensity analysis to unify measurements of size and stationar ity of land changes by interval, category,and transition. *Landscape and Urban Planning, 106*(1), 103-114. https://doi.org/10.1016/j.landurbplan.2012.02.010

Aniah, P., Bawaky, S., NiiArdey, S., & Mawunyo, F. (2023). Land use and land cover change detection and prediction based on CA-Markov chain in the savannah ecological zone of Ghana. *Environmental Challenges, 10,* 1–12.https://doi.org/10.1016/j.envc.2022.100664

Baidoo, R., Arko-Adjei, A., Poku-Boansi, M., Quaye-Ballard, A., & Somuah, P. (2023). Land use and land cover changes implications on biodiversity in the Owabi catchment of Atwima Nwabiagya North District,Ghana.*Heliyon,9*(5),e15238. https://doi.org/10.1016/j.heliyon.2023.e15238

Bailey, K., Mccleery, R., Binford, M., & Zweig, C. (2015). Land-cover change within and around protected areas in a biodiversity hotspot. *Journal of Land Use Science*,1-25. https://doi.org/10.1080/1747423X.2015.1086905

Belay,S., Amsalu, A., & Abebe, E. (2014). Land use and land cover changes in Awash National Park, Ethiopia: Impact of decentralization on the use and management of resources. *Open Journal of Ecology, 4,* 950–960. https://doi.org/10.4236/oje.2014.415079

Bieluczyk,W.,Merloti, F., Cherubin, R., Mendes, W., Bendassolli, A., Rodrigues, R., Camargo, B., van der, W., & Tsai, M. (2023). Forest restoration rehabilitates soil multifunctionality in riparian zones of sugarcane production landscapes. *Science of the Total Environment, 888*, 1-15. https://doi.org/10.1016/j.scitotenv.2023.164175

Congalton, R., & Green, K. (2008). *Assessing the accuracy of remotely sensed data: Principles and practices* (second edi). Taylor & Francis Group. http://www.taylorandfrancis.com/

Cunha, E., Santos, C., Silva, R., Bacani, V., & Pott, A. (2021). Future scenarios based on a CA-Markov land use and land cover simulation model for a tropical humid basin in the Cerrado/Atlantic Forest ecotone of Brazil. *Land Use Policy, 101*. https://doi.org/10.1016/j.landusepol.2020.105141

Debebe, B., Senbeta, F., Teferi, E., Diriba, D., & Teketay, D. (2023). Analysis of forest cover change and its drivers in biodiversity hotspot areas of the Semien Mountains National Park, Northwest Ethiopia. *Sustainability, 15,* 1-22. https://doi.org/10.3390/su15043001

Deribew, K. (2019). Spatially explicit statistical modeling of random and systematic land cover transitions in the main grassland plain of Nech Sar National Park, Ethiopia. *Ecological Processes, 8*(1), 1–20. https://doi.org/10.1186/s13717-019-0199-z

Feng, H., Wang, S., Zou, B., Nie, Y., & Ye, S. (2023). Land use and Cover change (LUCC) impacts on Earth's eco-envronments: Research progress and prospects. *Advances in Space Research, 71*(3), 1418–1435. https://doi.org/doi.org/10.1016/j.asr.2022.09.054

Fetene, A., Hilker,T., Yeshitela, K., Prasse, R., Cohen, W., & Yang, Z. (2015). Detecting trends in land use and land cover change of Nech Sar National Park, Ethiopia. *Environmental Management*, 137–147. https://doi.org/10.1007/s00267-015-0603-0

Franc, V., Zien, A., & Schölkopf, B. (2011).Support vector machines as probabilistic models. *Proceedings of the 28th International Conference on Machine Learning, 2011*, 665-672.

Gashaw, T., Tulu,T., Argaw, M., Worqlul, A., Tolessa, T., & Kindu, M. (2018). Estimating the impacts of land use/land cover changes on ecosystem service values:The case of the Andassa watershed in the upper Blue Nile basin of Ethiopia. *Ecosystem Services, 31*, 219-228.

https://doi.org/10.1016/j.ecoser.2018.05.001

Gidey, E., Dikinya, O., Sebego, R., Segosebe, E., & Zenebe, A. (2017). Cellular Automata and Markov Chain (CA-Markov) model-based predictions of future land use and land cover scenarios (2015-2033) in Raya, Northern Ethiopia. *Modeling Earth Systems and Environm ent*, *3*(4), 1245–1262. https://doi.org/10.1007/s40808-017-0397-6

Gui, W., Wen, Q., Dong, W., Zou, G., & Kong, D. (2025). Using natural vegetation succession to evaluate how natural restoration proceeds under different climate in Yunnan,Southwe st China.*PLoS ONE*, *20*, 1-21. https://doi.org/10.1371/journal.pone.0319420

Hailu, Y., Tilahun, B., Kerebeh, H., & Tafese, T. (2018). Land use land cover change detection in Gibe Sheleko National Park, Southwestern Ethiopia. *AgEcon*, *4*(4), 20–30.

Hyandye, C., & Martz, L.(2017). A Markovian and cellular automata land-use change predictive model of the Usangu Catchment. *International Journal of Remote Sensing*, *38*(1), 64–81. https://doi.org/10.1080/01431161.2016.1259675

Jin, Y., & Fan, H. (2018). *Land use/ land cover change and its impacts on protected areas in Mengla County, Xishuangbanna, Southwest China*. *2012*.

Kubiszewski, I., Costanza, R., Anderson, S., & Sutton, P. (2017). The future value of ecosystem services: Global scenarios and national implications. *Ecosystem Services*, *26*, 289–301. https://doi.org/10.1016/j.ecoser.2017.05.004

Kodero, M., Felzer, S., & Shi, Y.(2024). Future transition from forests to shrublands and grasslands in the Western United States is expected to reduce carbon storage.*Communic ations Earth and Environment*, *5*(1), 1-12. https://doi.org/10.1038/s43247-024-01253-6

Legesse, A. (2019). *CA-Markov Chain model based deforestation modeling in the lower catchment of Gidabo Basin*. Dilla University, Ethiopia.

Liping, C., Yujun, S., & Saeed, S. (2018). Monitoring and predicting land use and land cover changes using remote sensing and GIS techniques-A case study of a hilly area,Jiangle, China. *PLoS ONE*, *13*(7), 1–23. https://doi.org/10.1371/ journal.pone.0200493

Lu, X., Zhou, Y., Liu, Y., & Le, Y. (2018). The role of protected areas in land use/land cover change and the carbon cycle in the conterminous United States. *International Journal of Laboratory Hematology*, *38*(1), 42–49. https://doi.org/10.1111/ijlh.12426

Marchese, C. (2015). Biodiversity hotspots: A shortcut for a more complicated concept. *Global Ecology and Conservation*, *3*, 297–309. https://doi.org/10.1016/j.gecco.2014.12.008

Mathewos, M., Lencha, S., & Tsegaye, M. (2022). Land use and land cover change assessment and future predictions in the Matenchose Watershed, Rift Valley Basin, using CA-Markov Simulation. *Land*, *11*, 1–28. https://doi.org/10.3390/land11101632

Medina, A., Elena, B.,& Atehort, A. (2019). Comparison of maximum likelihood, support vector machines, and random forest techniques in satellite images classification. *Tecnura*, *23*(59), 13–26. https://doi.org/10.14483/22487638.14826

Mekonnen, M. (2022).*Human Activity, Biodiversity and Ecosystem Services in Protected Areas*. Springer NatureSwitzerland .https://doi.org/https://doi.org/10.1007/978-3-030-89571-6

Menbere, P. (2021). The implication of land use land cover change on biodiversity conservation: An overview from protected areas in Ethiopia. *Journal of Earth and Environmental Sciences Research*, *3*(2), 1–15. https://doi.org/10.47363/jeesr/2021(3)144

Muhammed, A., Bufebo, B., & Elias, E. (2016). Potential and threats on National Parks:The case of Nech Sar National Park. *Journal Of Harmonized Research*, *4*(4), 176–184.

NaughtonTreves, L., Holland, B., & Brandon, K. (2005). The role of protected areas in conservi ng biodiversity and sustaining local livelihoods. *Annual Review of Environment and Resources*, *30*, 219–252. https://doi.org/10.1146/annurev.energy.30.050504.164507

Nogueira, T., Ferreira, R., & Cortijo, D. (2014). Land Use Policy Land use changes in protected areas and their future : The legal effectiveness of landscape protection. *Land Use Policy*, *38*, 378–387. https://doi.org/10.1016/j.landusepol.2013.12.003

Nytch, C., Rojas, J., Erazo Oliveras, A., Santiago García, R., & Meléndez-Ackerman, E. (2023). Effects of historical land use and recovery pathways on composition, structure, ecological function, and ecosystem services in a Caribbean secondary forest. *Forest Ecology and Management*, *546*, 1-16. https://doi.org/10.1016/j.foreco.2023.121311

Pierce, N., Archer, S., Bestelmeyer, B., & James, D. (2019). Grass-Shrub competition in Arid lands:An overlooked driver in grassland-shrubland state transition? *Ecosystems*, *22*, 619–628. https://doi.org/10.1007/s10021-018-0290-9

Robson, A., Trimble, M., Bauer, D., Loveridge, A., Thomson, P., Western, G., & Lindsey, P. (2022). Over 80% of Africa's savannah conservation land is failing or deteriorating according to lions as an indicator species. *Conservation Letters*, *15*(1), 1-12. https://doi.org /10.1111/conl.12844

Sala, O., & Maestre, F. (2014). Grass-woodland transitions: determinants and consequences for ecosystem functioning and provisioning of services. *Journal of Ecology*, *102*(6), 1357-1362. https://doi.org/10.1111/1365-2745.12326

Shaar, W., Adjizian, J., Nabil, G., Hassan, N., Liliane, L., & Barakat, B. (2021). Application of modified cellular automata markov chain model: forecasting land use pattern in Lebano n. *ModelingEarthSystems andEnvironment*,*7*(2),1321-1335.https://doi.org/10.1007/s4080 8-020-00971-y

Shiferaw, H., Bewket, W., Alamirew, T., Zeleke, G., & Teketay, D. (2019). Implications of land use/land cover dynamics and Prosopis invasion on ecosystem service values in Afar Region, Ethiopia.*Scienceof the TotalEnvironment*,*675*,354-366. https://doi.org/10.1016/j.scitoten v.2019.04.220

Silva, I., Dupas, F., Costa, C., Medeiros, G., & de Souza, A. (2021). Spatiotemporal changes in land cover land use in protected areas of Serra da Mantiqueira, Southeastern Brazil. *Environmental Challenges*, *4*, 1–11. https://doi.org/10.1016/j.envc.2021.100195

Tadese, S., Soromessa, T., & Bekele, T. (2021). Analysis of the current and future Prediction of land use/land cover change using remote sensing and the CA-Markov model in Majang forest biosphere reservers of Gambella, Southwestern Ethiopia. *Scientific World Journal*, *2021*, 1–18. https://doi.org/https://doi.org/10.1155/2021/6685045

Tadesse, L.(2020). Application of remote sensing and geographical information system in mapping land cover of the national park. *Int. J. Hum. Capital Urban Manage*, *5*(2), 139-152. https://doi.org/10.22034/IJHCUM.2020.02.05

Temesgen, F., Bikila, W., & Hailemicael A. (2022). Seasonal land use/land cover change and the drivers in Kafta Sheraro national park, Tigray, Ethiopia. *Heliyon*, *8*(12), e12298. https://doi .org/10.1016/j.heliyon.2022.e12298

Tesfaw,T., Pfaff, A.,Golden, E.,Qin, S., & Medeiros, R. (2018). Land-use and land-cover change shape the sustainability and impacts of protected areas. *Proceedings of the National Academy of Sciences of the United States of America*, *115*(9),2084-2089. https://doi.org/ 10.1073/pnas.1716462115

Tsegaye, G., Dondeyne, S., Lemenih, M., Marye, A., Nyssen, J., Deckers, A., & Maertens, M. (2017).'Facing conservation or 'conservation with a human face'? People-park interaction s in southern Ethiopia. *Journal of Eastern African Studies*, *11*(2), 290-309. https://doi.org/ 10.1080/17531055.2017.1327167

Venter, O., Sanderson, W., Magrach, A., Beher, J., Jones, R., Possingham, P., Laurance, F.,Woo d, P., Fekete, M., Levy, A., & Watson, M. (2016). Sixteen years of change in the global terrestrial human footprint and implications for biodiversity conservation. *Nature Commu nications*, *7*, 1-11. https://doi.org/10.1038/ncomms12558

Verburg, H., Overmars, P., Huigen,A., Groot, D, & Veldkamp, A. (2006). Analysis of the effects of land use change on protected areas in the Philippines. *Applied Geography*, *26*, 153–173. https://doi.org/10.1016/j.apgeog.2005.11.005

Waseem,M., Halmy, A., Gessler, E., Hicke A., & Salem, B. (2015). Land use/land cover change detection and prediction in north-western coastal desert of Egypt using Markov-CA. *Applied Geography*, *63*, 101-112. https://doi.org/10.1016/j.apgeog.2015.06.015

Winkler, K., Fuchs, R., Rounsevell, M., & Herold, M. (2021). Global land use changes are four times greater than previously estimated. *Nature Communications*, *12*(1), 1-10. https://doi.org/10.1038/s41467-021-22702-2

Yesuph, A., & Dagnew, A. (2019). Land use/cover spatiotemporal dynamics, driving forces and implications at Beshillo catchment of Blue nile basin, Northeastern highlands of Ethiopia. *Environmental Systems Research*, *8*(1). https://doi.org/10.1186/s40068-0190148-y

Zadbagher, E., Becek, K., & Berberoglu, S. (2018). Modeling land use/land cover change using remote sensing and geographic information systems: case study of the Seyhan Basin, Turkey.*EnvironmentalMonitoringandAssessment*, *190* (8). https://doi.org/10.1007/s10661-018-6877-y

Zhang, Z., Hu, B., Jiang, W., & Qiu, H. (2021). Identification and scenario prediction of degree of wetland damage in Guangxi based on the CA-Markov model. *Ecological Indicators*, *127*, 107764. https://doi.org/10.1016/j.ecolind.2021.107764